Research Square

Preprints are preliminary reports that have not undergone peer review.
They should not be considered conclusive, used to inform clinical practice,
or referenced by the media as validated information.

Numerical Investigation on Effect of Confining Reinforcement on Post-Earthquake Fire Behavior of Reinforced Concrete Column

Selamawit Ayal Chanie

selamawit.ayal@uog.edu.et

University of Gondar

Tesfaye Alemu Mohammed

Addis Ababa Science and Technology University

Emebet Fentahun Ejigu

University of Gondar

Rakev Afework Weldemichael

University of Gondar

Getasew Kindie Mihiretu

University of Gondar

Yeshihareg Alelign Demissie

University of Gondar

Feven Tadese Geremew

University of Gondar

Research Article

Keywords: Post-earthquake fire, Finite element analysis and confining reinforcement

Posted Date: November 12th, 2026

DOI: https://doi.org/10.21203/rs.3.rs-11373130/v1

License: This work is licensed under a Creative Commons Attribution 4.0 International License.
Read Full License

Additional Declarations: No competing interests reported.

NUMERICAL INVESTIGATION ON EFFECT OF CONFINING REINFORCEMENT ON POST-EARTHQUAKE FIRE BEHAVIOR OF REINFORCED CONCRETE COLUMN

Selamawit Ayal Chanie[1]*, Tesfaye Alemu Mohammed[2,3], Emebet Fentahun Ejigu[1], Rakev Afework Weldemichael[1], Getasew Kindie Mihiretu[1], Yeshihareg Alelign Demissie[1], Feven Tadese Geremew[4]

[1]* Department of Civil Engineering, institute of technology, University of Gondar,196, Gondar, Ethiopia

[2] Department of Civil Engineering, Addis Ababa Science and Technology University, Addis Ababa, Ethiopia

[3] Construction Quality and Technology Center of Excellence, Addis Ababa Science and Technology University, Addis Ababa, Ethiopia

[4] Department of Hydraulic and Water Resource Engineering, University of Gondar,196, Institute of technology, Gondar, Ethiopia

*Correspondence author: Selamawit Ayal Chanie: selamawit.ayal@uog.edu.et, https://orcid.org/0009-0003-1058-9437

ABSTRACT

Intermediate tie reinforcement plays a vital role in enhancing the ductility of reinforced concrete columns (RC) by providing effective confinement to the core concrete and restraining the buckling of longitudinal reinforcement. Evaluating the residual load-carrying capacity of RC columns exposed to elevated temperatures following lateral loading. The effects of thermal stresses and deformations on the structural behavior of reinforced concrete columns subjected to fire following earthquake loading are not adequately addressed in conventional design codes. This study numerically investigates the effect of confining reinforcement on the post-earthquake fire behavior of RC columns. Specifically, the effects of confining tie configurations, concrete compressive strength, and transverse reinforcement spacing on column behavior under post-earthquake fire conditions are examined. A finite element model was developed using ANSYS Mechanical APDL 2020 R2 and validated against experimental results reported in the literature. The RC columns were modeled as cantilever members with 300*300 cross-sections. Following validation of the finite element model, a parametric study was conducted involving 19 finite element models.

The finite element analysis results show that reinforced concrete column with intermediate confining reinforcement improve the load carrying capacity by 12.48%. Intermediate confining ties increased load-carrying capacity by 4.98% under lateral loading and 11.48% under PEF loading, demonstrating greater effectiveness after fire exposure.

Due to the effect of thermal stress, load carrying capacities of the confined and unconfined column by intermediate ties were reduced by 6.38% and 12.5% respectively. Increasing spacing of transverse reinforcement from 100mm to 300mm (i.e. 66.66%) decreases the strength by 4.22%. In other way the strength of concrete increases from 23MPa to 45MPa (i.e. 95.6%), the load carrying capacity of the column was increased by 14.74%.

Keywords: Post-earthquake fire, Finite element analysis and confining reinforcement

1. Introduction

Reinforced concrete columns (RC) are one of the main structural members in buildings. They carry vertical loads and bending moments from corresponding floors and beams. It is most likely designed to carry axial loads and lateral loads from earthquakes and wind. Like earthquakes, fire is considered one of the hazardous which seriously affect the safety of the reinforced concrete structures. Adequate confinement of the concrete core and effective restraint of longitudinal reinforcement by transverse ties improve the strength, ductility, and deformation capacity of RC columns.

Understanding the behavior of structures subjected to fire, particularly post-earthquake fire (PEF), has become an important area of research due to the increasing concern over multi-hazard events. Earthquakes are unpredictable natural hazards that can cause significant damage to structural components, while fire poses a serious threat to building integrity and human safety, particularly when it occurs following an earthquake. Such events can lead to substantial loss of life and considerable economic damage. The combined effects of earthquake-induced structural damage and subsequent fire exposure can significantly compromise the strength, stiffness, and stability of reinforced concrete structures. Therefore, comprehensive investigations into the behavior of RC structures under post-earthquake fire conditions are essential for assessing their structural performance and ensuring adequate safety and resilience.

Vitorino et al. (2020) reported that post-earthquake fires can occur following major earthquakes and may, under certain circumstances, cause consequences more severe than those of the earthquake itself. Such events in urban environments can result in substantial losses of human life and property. Their findings indicate that earthquake-induced damage can compromise the fire resistance of reinforced concrete structures, particularly when concrete cover is lost, exposing the reinforcing steel directly to elevated temperatures. This highlights the importance of considering the effects of prior seismic damage when evaluating the fire resistance and post-earthquake fire performance of RC structural elements. Behnam and Ronagh (2013) identified fire following earthquake as a significant risk to structures already weakened by seismic damage, as subsequent fire exposure may accelerate structural deterioration and lead to premature collapse. They

recommended that fire safety regulations account for seismic risk by incorporating appropriate fire-resistance requirements for buildings in earthquake-prone regions.

The modern construction standards give design value to have adequate resistance against an expected level of earthquake and fire resistance of reinforced concrete column. Existing studies have mainly examined the seismic behavior and fire resistance of reinforced concrete columns separately, rather than considering them together. To overcome the effects of the post-earthquake fire, more parametric studies are required. Although some researchers have recommended post-earthquake fire resistance requirements for specific building members, their focus has been limited to certain parameters. In particular, previous studies have primarily considered the depth of the concrete cover when examining post-earthquake fire effects on structural elements. Thus, there is a research gap on confining reinforcement and tie configuration to determining the effect of fire after earthquake on RC columns.

To addresses these gaps by developing and validating a nonlinear FE model capable of simulating sequential seismic and fire loading on RC columns. To validate 3D coupled thermal mechanical FE model against full-scale experimental results. The specific objectives are to evaluate the effects of confining reinforcement tie configurations, transverse reinforcement spacing, and concrete strength on the load–displacement response, concrete damage, and ductility of reinforced concrete columns under post-earthquake fire loading.

2. Literature review

Imani et al. (2015) investigated the behavior of concrete-filled double-skin tube columns subjected to fire after simulated seismic loads. Three identical columns were tested in two phases: static lateral loading and fire exposure. One column was tested under fire in an undamaged state, while the other two were first subjected to lateral drifts of 6–6.5% to simulate moderate and high seismic damage, with residual drifts of 1.4% and 3.9%, respectively. All columns were then exposed to ISO-834 standard fire under axial load until failure, during which local buckling of the tubes occurred due to thermal expansion and separation from the concrete.

Behnam B. et al. (2015) noted that concrete and reinforcement exhibit different thermal behaviors at elevated temperatures, leading to varying thermal stresses until degradation occurs. While

concrete has low thermal conductivity, reinforcement has high conductivity, but it is normally protected by the concrete cover. However, after lateral loading, the concrete cover may crack, exposing the reinforcement directly to fire and increasing structural damage.

Kunnath et al. (2017) investigated the cyclic behavior of reinforced concrete columns exposed to both fire and earthquake loading, considering varying hoop spacing and longitudinal bar diameters. In their study, one specimen was subjected only to cyclic loading, while another experienced both seismic and high-temperature loading according to a standard fire. The results showed severe spalling of the concrete cover during fire, along with reductions in strength, ductility, and stiffness compared to columns not exposed to fire. Columns with smaller-diameter longitudinal bars and better confinement demonstrated improved seismic performance. Both specimens failed in a similar manner, with final failure caused by buckling of the longitudinal steel bars and crushing of the confined concrete core.

Chinthapalli and Agarwal (2020) studied the effect of confining reinforcement on the fire behavior of reinforced concrete columns, considering different concrete strengths (M30 and M50), heating durations (140 and 200 minutes), and volumes of confining reinforcement (0.25% and 2.14%). They concluded that increasing the confining reinforcement from 0.25% to 2.14% raised the axial load–carrying capacity of columns at elevated temperatures by 75%. However, extending the fire duration from 140 to 200 minutes reduced the load-carrying capacity by 44%. Additionally, higher concrete grades positively influenced the axial load–carrying capacity under elevated temperatures.

Demir et al. (2020) conducted an experimental study on the post-fire seismic behavior of reinforced concrete columns, focusing on concrete cover thickness (25 and 40 mm) and fire durations (30, 60, and 90 minutes). The columns were tested under constant axial load and cyclic lateral displacement following exposure to standard fire. The study evaluated lateral load–displacement response, ductility, stiffness, energy dissipation, and residual displacements. The results showed that fire exposure reduced the columns' lateral load capacity, while concrete cover thickness had only a minor effect on post-fire seismic behavior.

Vitorino et al. (2022) investigated the post-earthquake fire performance of reinforced concrete (RC) frame structures using numerical models developed with SAFIR. After validating the modelling approach, the researchers performed a parametric study considering different earthquake-induced damage locations and configurations and different fire locations. The results showed that earthquake-damaged RC frames had lower fire resistance than undamaged frames, with heavily damaged frames potentially collapsing more than 2 hours earlier. The study demonstrated that earthquake damage can significantly increase the vulnerability of RC structures to subsequent fire, particularly when emergency response and rescue operations are delayed.

Raut et al. (2013) conclude that high strength concrete (HSC) columns exhibit lower fire resistance, as compared to conventional normal strength concrete columns, due to occurrence of fire induced spalling and faster degradation of strength and stiffness properties of concrete with temperature.

Shanan et al. (2019) conducted the capacity of normal and high strength reinforced concrete columns which confined with transverse steel under compressive loading. The parameters of the study were concrete strength, volumetric ratio, spacing of transverse reinforcement, longitudinal reinforcement distribution and yield strength of transverse reinforcement. The results indicated that both strength and ductility of confined concrete increase with increasing the volumetric ratio of confinement.

Hazem M. Elbakry et al. (2024) performed a numerical study to evaluate the influence of internal tie configurations on the axial behavior of reinforced concrete columns. The results revealed that columns reinforced with V-shaped ties exhibited superior confinement efficiency, higher axial load capacity, and improved resistance to longitudinal reinforcement buckling compared with those reinforced using conventional cross-ties. Additionally, the study concluded that closer transverse reinforcement spacing significantly enhanced the strength, ductility, and overall performance of the columns.

According to Shiwen et al. (2024), the influence of FRP tie parameters on the behavior of concrete columns was investigated. The results demonstrated that tie configuration and spacing significantly affected confinement effectiveness, load-carrying capacity, and ductility. The study

revealed that closed-type FRP ties enhanced concrete confinement and improved the overall structural performance of reinforced concrete columns.

3. Material and Methodology

The nonlinear finite element simulations in this study were performed using ANSYS Mechanical APDL 2020 R2. The FE model represents the material behavior of concrete and reinforcing steel, together with the applied boundary conditions and material-specific failure criteria, to predict the structural response of reinforced concrete columns.

3.1. Overview of Numerical Modelling Approach

A three-dimensional (3D) finite element model was developed using ANSYS Mechanical APDL 2020 R2 to investigate the behavior of a reinforced concrete column exposed to the ISO 834 standard fire. Following fire exposure, the column was subjected to sustained axial loading and lateral loading to evaluate its structural response. The model geometry, material properties, boundary conditions, and loading protocol were adopted from the full-scale experimental study of Demir et al. (2020) to validate the numerical model against experimental results.

3.2 Geometry and Reinforcement Details

The validated FE model was developed based on the experimental RC column tested by Demir et al. (2020). As shown in Fig. 1 and Table 1, the numerical model reproduced the experimental geometry, including the 300 × 300 mm cross-section, 1500 mm height, 20 mm longitudinal bars, and 10 mm stirrups spaced at 100 mm, ensuring consistency between the numerical and experimental specimens. The material properties adopted for the FE model are summarized in Table 2, including the mechanical properties of concrete and reinforcing steel, while concrete density and emissivity were included for the thermal analysis. These parameters provide a consistent basis for FE model validation.

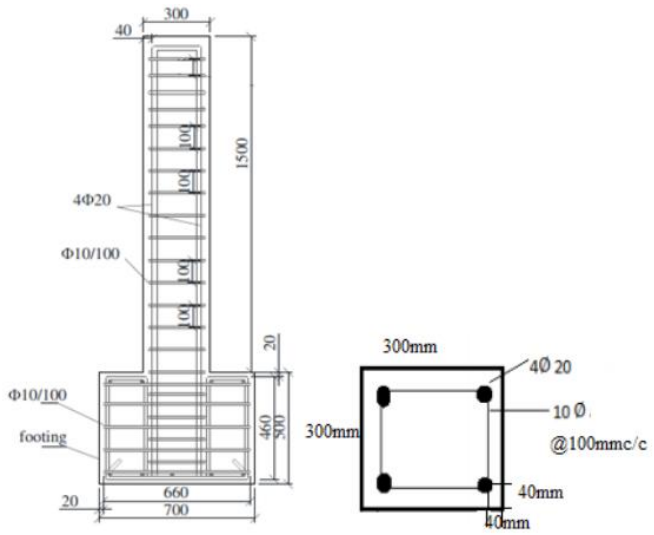


Fig.1 Elevation; and plan views of reinforcement and cross-section detail (source: Demir et al.2020)

Table 1 column cross-section details (source: Demir et al. 2020)

Type	Sub Type	Values (mm)
Cross Section	Height	1500
	Width	300
	Depth	300
Longitudinal Bar	Diameter	20
Stirrups	Diameter	10
	Spacing	100

Material properties		
Concrete property	**Value**	**Unit**
Average Compressive strength	36	Mpa
Modulus of elasticity at normal temperature	28200	Mpa
Poisson's ratio	0.2	-
Emissivity	0.7	-
Density	2500	Kg/m3

Reinforcing steel property	**Value**	**Unit**
Modulus of elasticity at normal temperature	200000	Mpa

Poisson's ratio	0.3	-
Average yield strength for main bar	461	Mpa
Average yield strength for hoops	472	Mpa

Following model validation, a parametric study was carried out to investigate the effect of different confining tie configurations on the post-fire behavior of the columns. To accommodate the additional confining ties, four extra longitudinal reinforcement bars were introduced. As shown in Fig. 2 to maintain approximately the same total longitudinal reinforcement area as the validated specimen, the diameter of the longitudinal bars was reduced from 20 mm to 14 mm.

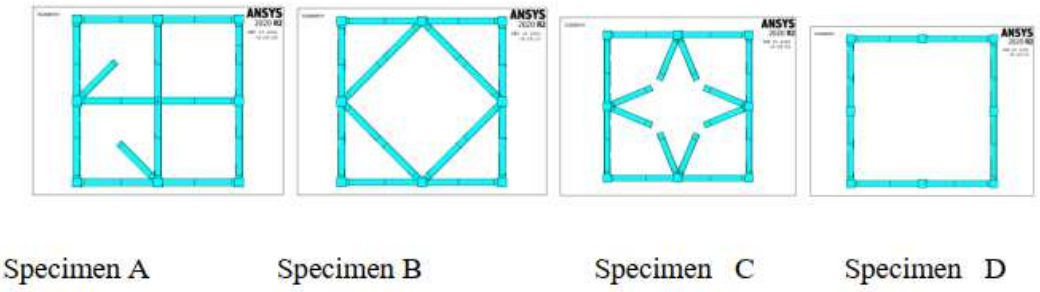


Fig. 2 Details and layout of intermediate tie configurations

3.3 Element Types and Material Models

The finite element model consisted of the following components:

I. **Concrete:** Modeled using CPT215 solid elements with a coupled damage-plasticity formulation to accurately simulate cracking, crushing, and stiffness degradation under combined thermal and mechanical loading.

II. **Steel reinforcement:** Modeled using REINF264 truss elements with a bilinear isotropic hardening material model to represent the nonlinear behavior of reinforcing steel.

III. **Thermal analysis:** Performed using SURF152 surface effect elements to apply the ISO 834 standard fire exposure to the column surfaces. Temperature-dependent thermal and mechanical properties were assigned to both concrete and reinforcing steel in accordance with the reduction factors specified in Eurocode 2 (EN 1992-1-2).

3.4 Loading and boundary conditions

To ensure that the model acts in the same way as the experimental specimen, loading protocol, material type and boundary conditions are needed to be applied where the supports and loads exist. The supports were modeled as a fixed support at the bottom and free end at the top. i.e. the column was restrained at the bottom and all DOF set as zero. Column that subjected to constant axial load and lateral displacement before exposed to ISO-834 standard fire. Applying the axial load, lateral displacement had been imposed using hydraulic actuators connected to the column loading head (Demir et al. 2020). The loading sequence adopted in the finite element analysis consisted of the following stages:

I. **Seismic stage:** A constant axial load was first applied to the reinforced concrete column, followed by cyclic lateral displacement loading with a maximum displacement of 96 mm to simulate earthquake-induced damage.

II. **Fire stage:** After completion of the seismic loading, the damaged column was exposed to the ISO 834 standard fire for 30 minutes. The resulting temperature distribution was subsequently transferred to the structural analysis through a one-way coupled thermo-mechanical procedure to evaluate the post-earthquake fire behavior of the column.

3.5 Parametric Study

This study used finite element analysis to investigate the effects of key parameters, including concrete strength, confining tie configuration, and transverse reinforcement spacing, on the behavior of reinforced concrete columns under post-earthquake fire (PEF) conditions. After validation, the model was used to investigate:

I. Strength of concrete (23, 36 45Mpa)
II. Confining tie configuration
III. Transverse reinforcement spacing (100mm, 200 and 300m)

The parametric study summarized in Table 3 was designed to systematically evaluate the effects of tie configuration, transverse reinforcement spacing, and concrete compressive strength on the lateral load response of RC columns. A total of 16 analyses were considered to enable direct

comparison between the reference specimen and the selected parameter variations. The investigated ranges were selected to represent practical reinforcement configurations and different concrete strength levels. The effects of these parameters on the lateral load carrying capacity, ductility, stiffness degradation, and damage behavior of reinforced concrete (RC) columns were investigated.

Table 2. Parametric Study Models and Parameter Combinations for Post-Earthquake Fire (PEF) Analysis

Parameters		Column Specimen / Variable	Number of Analyses
I.	Tie configuration	Specimen A (Sv = 100 mm, f'c - 36 MPa)	16
		Specimen B (Sv = 100 mm, f'c -36 MPa)	
		Specimen C (Sv = 100 mm, f'c -36 MPa)	
		Specimen D (Sv = 100 mm, f'c -36 MPa)	
II.	Spacing of transverse reinforcement	Specimen A with Sv = 200 mm; f'c -23, 36, and 45 MPa	
		Specimen A with Sv = 300 mm; f'c -23, 36, and 45 MPa	
III.	Concrete strength	Specimen A with f'c -23 MPa; Sv = 100, 200, and 300 mm	
		Specimen A with f'c -45 MPa; Sv = 100, 200, and 300 mm	

Table 3. Parametric Study Models and Combinations for lateral loading Analysis

Parameter	Column Specimen / Variable	Number of Analyses

Tie configuration	Specimen A with Sv = 100, 200, and 300 mm; f'c - 36 MPa	
	Specimen B with Sv = 100 mm; f'c - 36 MPa	5
	Specimen C with Sv =100 mm; f'c -36 MPa	

4. Results and discussion

In this section, finite element analysis (FE) was used to validate the model and investigate parametric effects on reinforced concrete columns. The column used for validation was also adopted as the reference specimen for the parametric study; however, in this case, the specimen was modeled without confining ties, and its behavior was evaluated in terms of peak lateral load, ductility, and damage. Based on the comprehensive numerical analysis, the study yielded significant findings on the behavior of reinforced concrete columns under post-earthquake fire (PEF), which are summarized below.

4.1 Validation Results of the Finite Element Model

Experimental results from Demir et al. were used to validate the nonlinear finite element model developed in ANSYS Mechanical APDL for reinforced concrete columns under post-earthquake fire conditions. The validation compared the numerical and experimental load–displacement responses for a 30-minute fire exposure, 40 mm concrete cover, and 84 mm displacement. As presented in Table 4 and Fig. 3, the FE model showed good agreement with the experimental results, with only a 5.67% difference in load capacity. The numerical model also reproduced the experimental response in terms of initial stiffness, peak lateral load, and post-peak behavior, confirming its suitability for the subsequent parametric analysis.

Table 4. Comparison of FEA with experimental result

Value	**Pmax (KN)**
Experimental result (Demir et al. 2020)	110.21
Numerical result	116.84

Different in % between experimental and numerical	5.67%

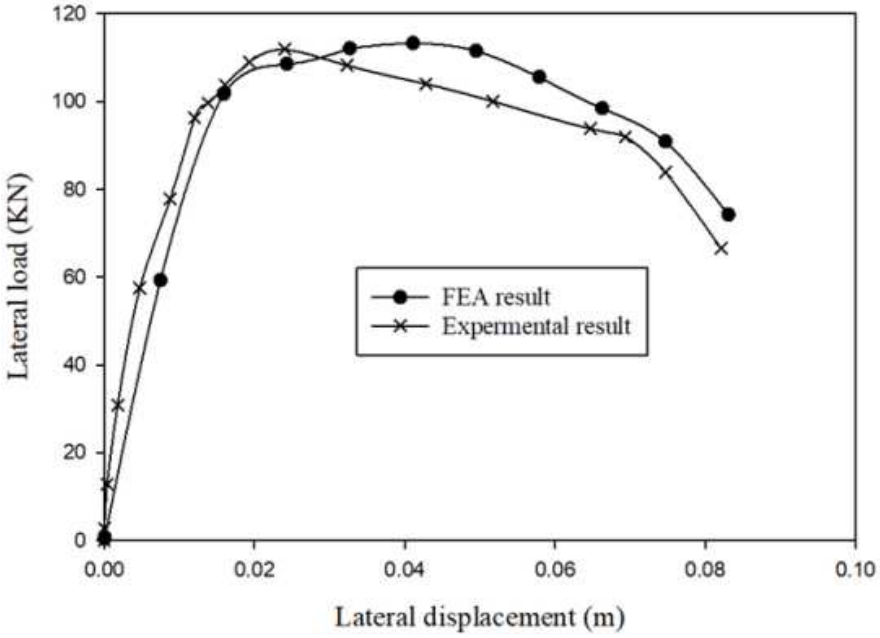


Fig. 3 Lateral load-lateral displacement curves for the FE analysis and experimental results

I. Damage mode of validation column

As shown in Fig. 4, the validation analysis indicated that the RC column failed mainly in a flexural mode as evidenced by cracking of concrete in the tension zone and crushing of concrete near the compression face. Spalling of the concrete cover and yielding of the longitudinal reinforcement were concentrated in the plastic hinge regions. These damage patterns were very similar to the experimental observations, which verified that pre-existing seismic cracks indeed accelerated heat penetration and material degradation during post-earthquake fire exposure, resulting in reduced residual strength and stiffness.

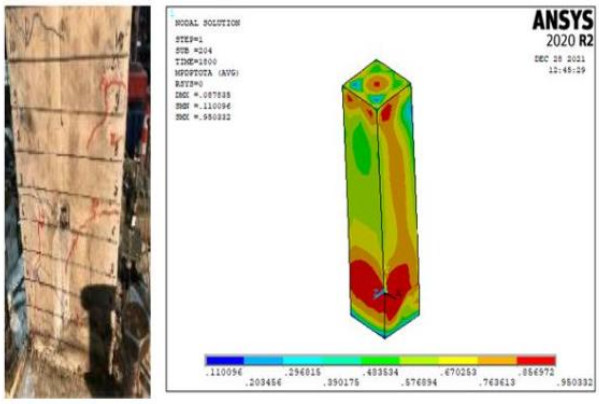


Fig. 4 Reinforced concrete column damage of experimental and FEA Resul

4.2. Finite element parametric study

Finite element analysis was performed to investigate the effects of concrete strength, confining tie configurations, and transverse reinforcement spacing on reinforced concrete columns under post-earthquake fire loading. The column responses were evaluated using lateral load–displacement behavior, concrete damage, and ductility. The analysis maintained constant parameters of 40 mm concrete cover, four-side fire exposure, and 30-minute fire duration. The validated column model without confining ties was used as the reference specimen for the parametric study.

4.2.1. Effect of configurations of confining reinforcements

I. Lateral load-lateral displacement relationships

To investigate the effect of confining ties on reinforced concrete (RC) columns subjected to post-earthquake fire (PEF), four additional 14 mm longitudinal reinforcing bars were introduced to maintain an equivalent reinforcement area. All parametric analyses were conducted on confined RC columns with three confining tie configurations (Specimens A, B, and C), as illustrated in Fig. 2. The influence of tie configuration was evaluated while keeping the transverse reinforcement spacing and concrete strength constant. The ultimate load-carrying capacity was obtained from the finite element (FE) load–displacement curves (Fig. 5). Under PEF loading, the residual ultimate load capacities of Specimens A, B, and C were 141.136 kN, 138.789 kN, and 137.711 kN, respectively, compared with 125.471 kN for the unconfined reference column. This represents increases of 12.48%, 10.61%, and 9.75%, respectively. Under lateral loading without fire exposure, the corresponding ultimate load capacities were 150.49 kN, 148.16 kN, and 147.09 kN, while the reference column reached 143.36 KN. Intermediate confining ties increased load-carrying capacity by 4.98% under lateral loading and 11.48% under PEF loading, demonstrating greater effectiveness after fire

exposure. Although all specimens exhibited similar initial stiffness up to yielding, Specimen A achieved the highest ultimate load capacity, while the unconfined reference column experienced the greatest strength loss.

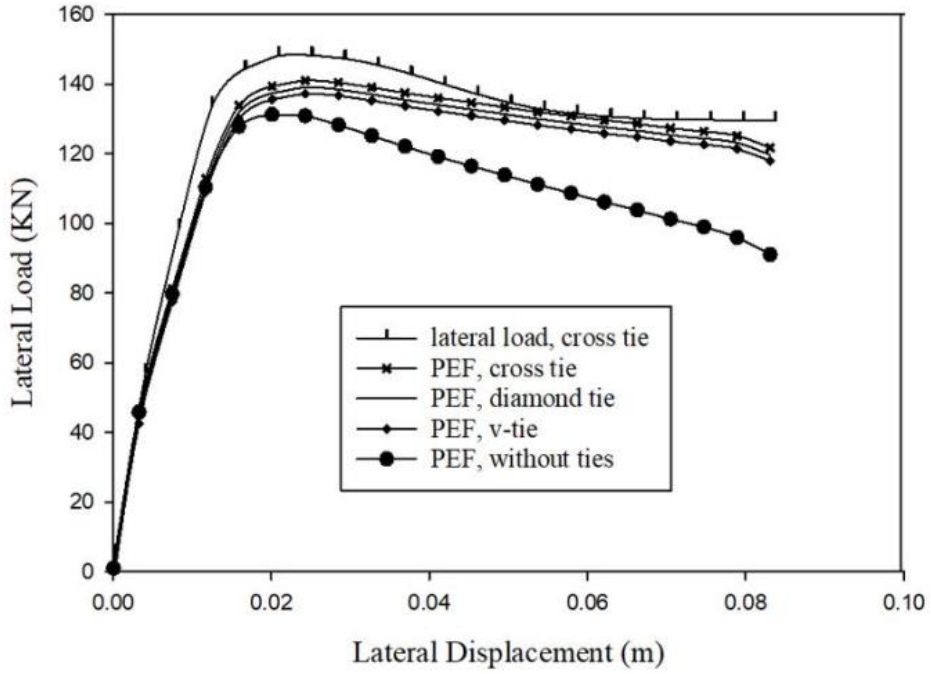


Fig. 5 Lateral load-lateral displacement relations for specimen A, B and C

II. Damage of concrete

The total micro-plane damage (compression, tension, and microcracks) in the reinforced concrete columns is represented by different color regions corresponding to the scalar isotropic damage variable in the coupled damage-plasticity micro-plane model. Red color indicates highly damaged regions, yellow color indicates moderate damage, green color indicates minor damage, and blue color represents negligible damage. As shown in Fig. 6, the extent and distribution of damage vary with the configuration of the confining ties. The column confined with V-ties exhibits greater damage than those confined with cross and diamond ties. However, the temperature distribution remained the same for all specimens (Fig. 7), as it primarily depends on the concrete cover thickness and the duration of fire exposure.

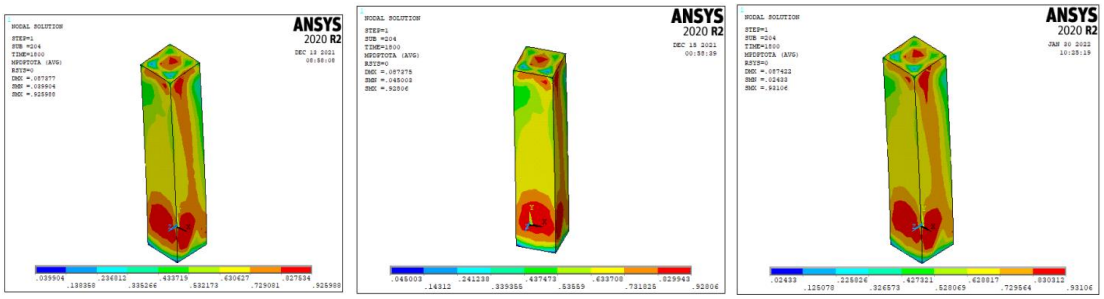


Fig. 6. Total concrete damage of the columns with different configuration of confining ties

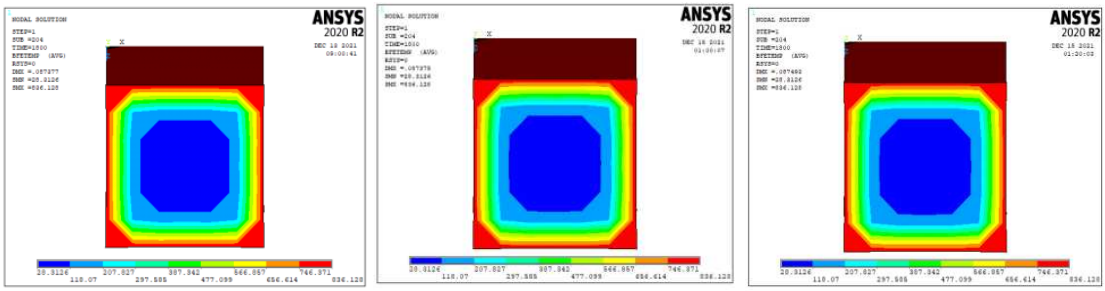


Fig. 7 Temperature distributions of columns with different configuration of confining ties

III. Ductility

The ductility behavior of reinforced concrete columns varies depending on the configuration of the confining ties. As shown in Table 5, the unconfined reinforced concrete column exhibited the lowest ductility compared with all confined specimens, indicating the significant contribution of transverse confinement to ductile performance.

The result suggests that the differences in damage, ductility, and confinement effectiveness were primarily governed by the geometry of the transverse reinforcement rather than the thermal exposure, since all specimens had identical concrete cover thicknesses and fire durations and exhibited similar temperature distributions. The diamond and V-shaped tie configurations provided more effective restraint to the longitudinal reinforcement and concrete core, thereby reducing bar buckling, limiting lateral expansion of the core, and enabling the columns to sustain larger deformations before failure. Although the V-tie-confined column exhibited greater localized concrete damage, this may be attributed to the concentration of stresses around the tie intersections and anchorage regions. Such localized damage did not necessarily indicate inferior confinement;

instead, the V-tie configuration was still able to maintain effective core confinement and longitudinal-bar restraint, contributing to higher ductility compared with the cross-tie configuration. In this study, the ductility ratio (μ) was evaluated from the load-displacement curves obtained from the finite element analysis (FEA). It was calculated as the ratio of the ultimate displacement (Δu) to the yield displacement (Δy), as given in Equation 1.

$$\mu = \frac{\Delta u}{\Delta y} \quad \text{..... Equation 1}$$

where; μ = displacement ductility ratio

Δu = ultimate displacement

Δy = yield displacement

Table 5. ductility ratios for different configurations

Specimen	Ultimate Displacement, Δu (mm)	Yield Displacement, Δy (mm)	Ductility Ratio, μ	% Difference
A	84.00	11.70	7.18	1.70
B	84.00	11.45	7.34	3.97
C	84.00	11.45	7.34	3.97
D (Reference)	84.00	11.90	7.06	Reference

4.2.2. Effect of grade of concrete

I. Lateral load-lateral displacement relationships

The effect of concrete strength on the load-carrying capacity, ductility, and damage behavior of reinforced concrete columns was investigated using three concrete grades: f'c - 23 MPa, 36 MPa, and 45 MPa. The analysis was conducted on the same column specimen (Specimen A) with a

transverse reinforcement spacing of 100 mm. The results demonstrate as shown in Fig. 8, increasing concrete strength enhanced the load-carrying capacity of the reinforced concrete columns both before and after thermal exposure. Before thermal exposure, increasing the concrete compressive strength from 23 MPa to 45 MPa increased the peak load from 135.578 kN to 160.896 kN, representing an 18.67% increase. This improvement can be attributed to the higher compressive strength of the concrete, which enables the column to sustain greater compressive stresses before significant damage and failure occur.

The beneficial effect of higher concrete strength was also maintained after thermal exposure. The residual load-carrying capacity increased from 128.984 kN for the 23 MPa concrete to 147.997 kN for the 45 MPa concrete, corresponding to a 14.74% increase. Although thermal exposure reduced the load-carrying capacity of columns, the higher-strength concrete retained a greater residual capacity. However, the percentage reduction in capacity due to thermal exposure increased with concrete strength, from 4.86% for 23 MPa concrete to 6.22% and 8.02% for 36 MPa and 45 MPa concrete, respectively. This trend indicates that higher-strength concrete was relatively more sensitive to thermal exposure. This behavior may be associated with its denser microstructure and lower permeability, which can restrict moisture and vapor movement during heating and consequently increase internal pore pressure and thermal-induced damage.

Despite the greater relative reduction in capacity, the 45 MPa concrete still exhibited the highest residual load-carrying capacity after thermal exposure. The increase in capacity provided by increasing the concrete strength from 23 MPa to 45 MPa decreased from 18.67% before thermal exposure to 14.74% after thermal exposure. This reduction indicates that thermal degradation partially diminished, but did not eliminate, the mechanical advantage associated with higher concrete strength. Therefore, the results should not be interpreted as indicating that the 45 MPa concrete performed worse than the 23 MPa concrete after fire exposure. Rather, the higher-strength concrete maintained the highest absolute load-carrying capacity, while experiencing a greater percentage loss relative to its initial capacity.

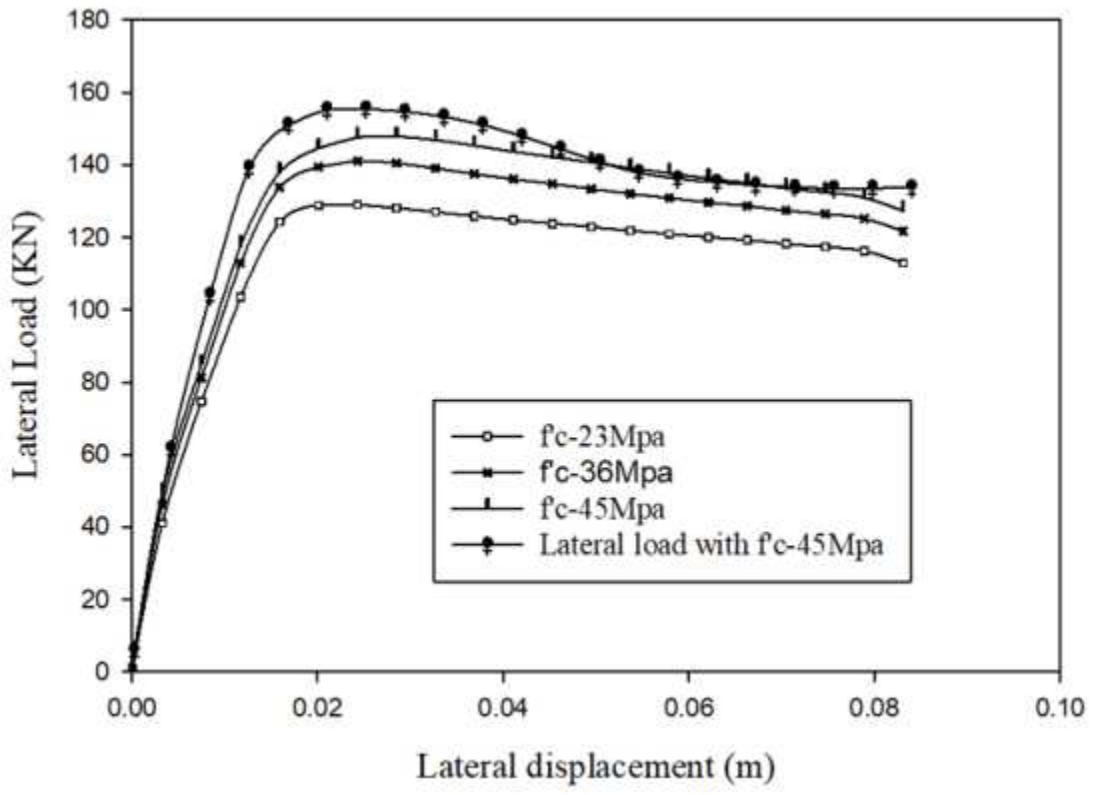


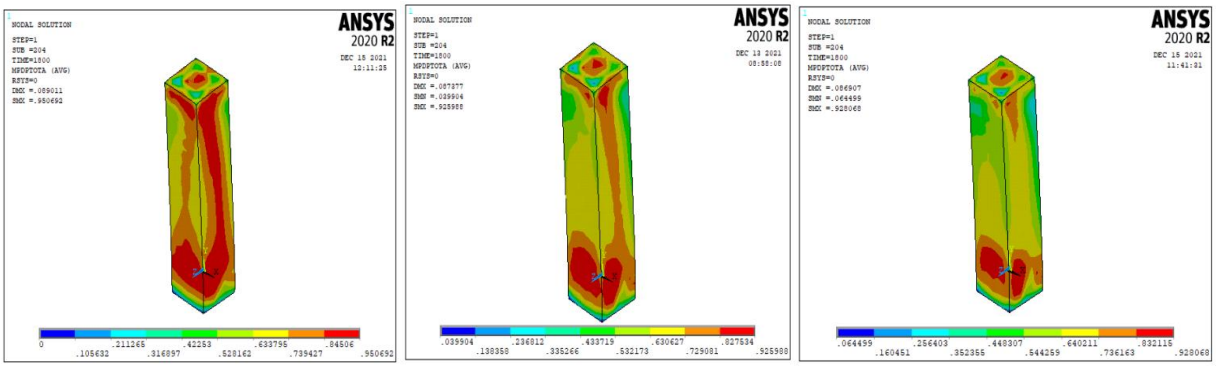
Fig. 8 Effect of strength of concrete on Lateral load- lateral displacement relationships

II. Damage of Concrete

As shown in Fig. 9, the extent and distribution of concrete damage are strongly influenced by the concrete compressive strength. The column with a concrete compressive strength of (f'c - 23) MPa exhibited the most extensive damage, as evidenced by the larger areas of red-colored regions in the damage contours. This indicates a higher level of concrete deterioration compared with the columns having (f'c -36) MPa and (f'c -45) MPa. The greater damage observed in the lower-strength concrete can be attributed to its lower resistance to thermally induced stresses and mechanical degradation under elevated temperatures. As the concrete strength increases, its ability to resist compressive stresses and maintain structural integrity during thermal exposure improves, resulting in a reduction in the extent and severity of damage.

In contrast, the temperature distribution was nearly identical for all grades of concrete. This similarity is expected because the specimens were subjected to the same fire exposure duration and had identical concrete cover thickness and thermal conductivity. Therefore, the differences in

damage patterns cannot be attributed to variations in temperature distribution but primarily to the different mechanical properties associated with the concrete grades



a/ concrete damage (f'c-23Mpa) b/ concrete damage (f'c-36Mpa) c/ concrete damage (f'c-45Mpa)

Fig. 9 Total damage of the columns with different grade of concrete

III. Ductility

The results indicate that increasing the concrete compressive strength slightly reduces column ductility due to the more brittle behavior of higher-strength concrete. As shown in Table 6, the ductility ratio decreases from 7.22 for 23 MPa concrete to 7.13 for 45 MPa concrete, indicating that the effect of concrete strength on ductility is relatively small.

The slight reduction in ductility with increasing concrete compressive strength can be attributed primarily to the reduced deformation capacity and more brittle post-peak behavior of higher-strength concrete. As the concrete strength increases, the concrete can sustain higher compressive stresses but generally undergoes lower ultimate compressive strains, resulting in reduced deformation capacity after peak load. However, because the observed reduction in ductility ratio is only about 1.25%, the influence of concrete strength on the overall column ductility is relatively minor.

Table 6. Ductility Ratios for Different Grades of Concrete

Strength of concrete (MPa)	Δu (mm)	Δy (mm)	μ = Δu/Δy
f'c-23	84	11.634	7.22
f'c-36	84	11.700	7.18
f'c-45	84	11.782	7.13

4.2.3. Effect of spacing of transverse reinforcement

I. Lateral Load–Lateral Displacement Relationships

The effect of transverse reinforcement spacing on the lateral load-carrying capacity and post-earthquake fire (PEF) behavior of the RC column was evaluated using lateral load–lateral displacement relationships. The column geometry and specimen type (Type A) were kept constant, while the concrete compressive strength (f'c - 23, 36, and 45 MPa) and the spacing of the hoops and tie reinforcement (100, 200, and 300 mm) were varied.

As shown in Fig. 10, under PEF conditions, increasing the transverse reinforcement spacing from 100 mm to 300 mm, corresponding to a 66.67% increase, resulted in reductions in the peak load capacity of 4.22%, 4.33%, and 4.47% for concrete strengths of 23, 36, and 45 MPa, respectively. As shown in Table 8, under lateral loading, the same increase in spacing reduced the column load-carrying capacity by 6.52% for 36 MPa concrete. These results indicate that increasing the transverse reinforcement spacing reduces the load-carrying capacity of the reinforced concrete column, with the reduction being more pronounced under lateral loading.

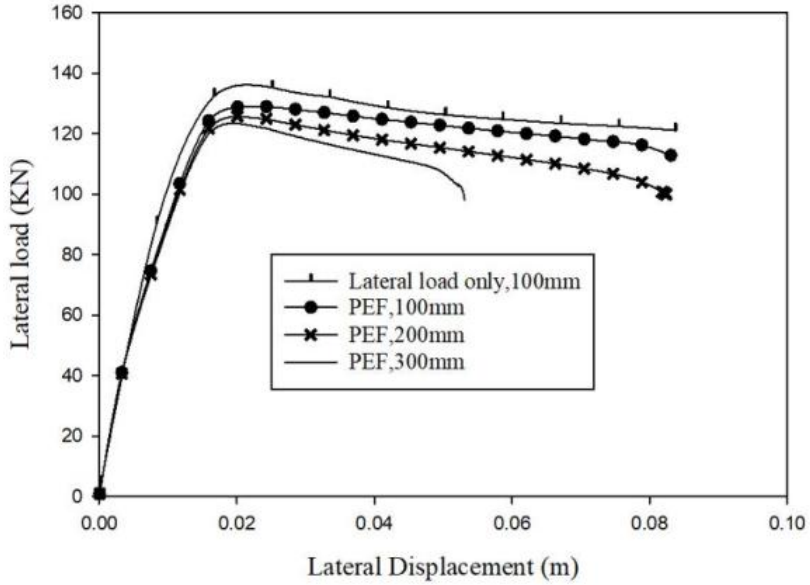


Fig. 10 Lateral Load-Lateral displacement relationships with different spacing of transverse reinforcement (f'c-23Mpa)

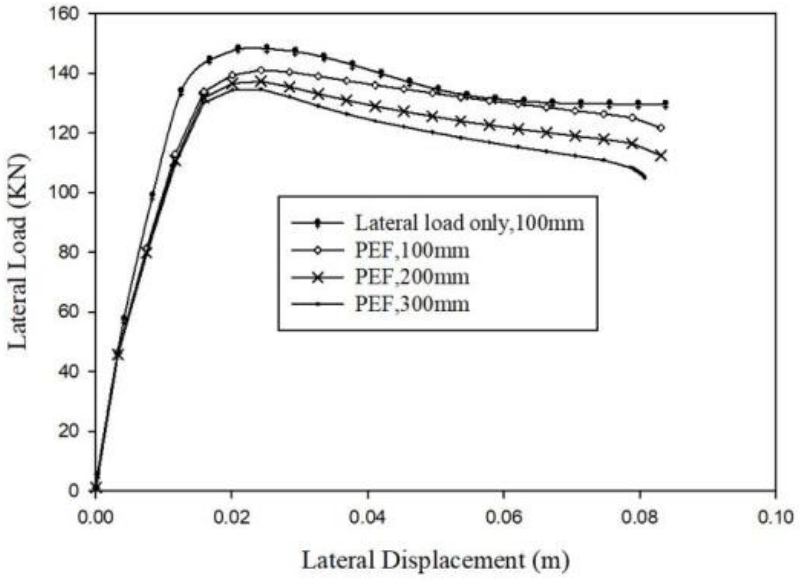


Fig. 11 Lateral Load-Lateral displacement relationships with different spacing of transverse reinforcement (f'c-36Mpa)

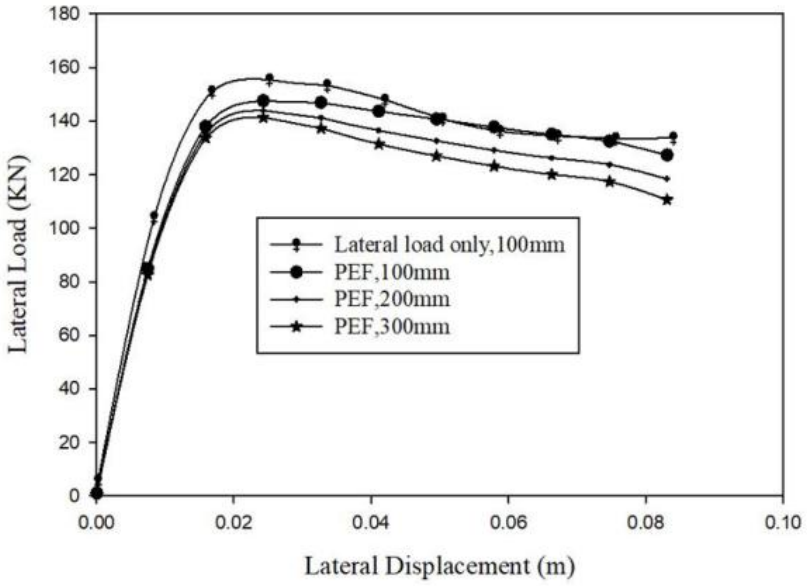


Fig. 12 Lateral Load-Lateral displacement relationships for specimen type A with different spacing of transverse reinforcement (f'c-45Mpa)

As shown in Fig. 11 and 12, the lateral load-carrying capacity decreases as the spacing of transverse reinforcement increases. Accordingly, the column subjected to PEF with 300 mm transverse reinforcement spacing exhibits lower load-carrying capacity than those with 100 mm and 200 mm spacing. This behavior is associated with the reduced confinement provided by the transverse reinforcement at larger spacing. When the amount of transverse reinforcement is reduced, the confinement of the concrete core becomes less effective, which can lead to increased concrete brittleness and reduced ductility and load-carrying capacity. The peak load and ductility differences among the specimens with different transverse reinforcement spacing are presented both in Table 7, 8 and 9 respectively.

Table 7 Peak lateral load resistance of columns with different spacing of transverse reinforcement (f'c-23Mpa)

Spacing of transverse reinforcement (mm)	Capacity of column (KN)	Percentage difference
100	128.984	reference

200	125.81	2.46
300	123.546	4.22

Table 8 Peak lateral load resistance of columns with different spacing of transverse reinforcement (f'c-36Mpa)

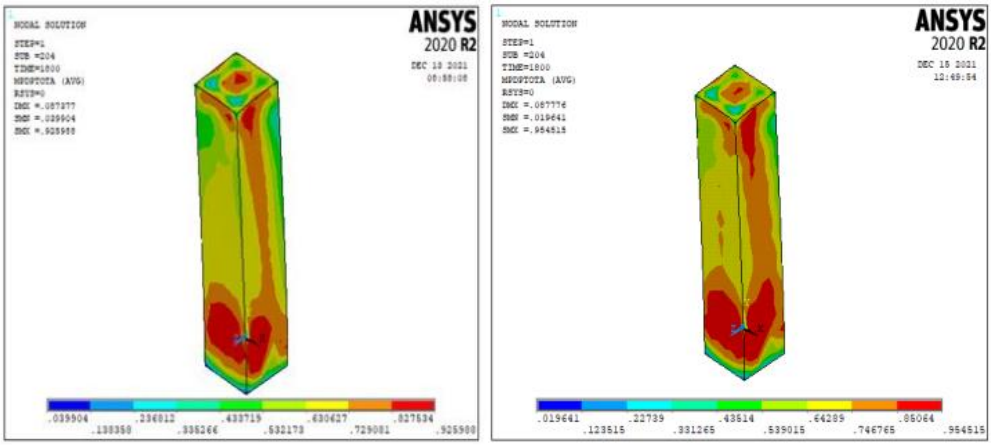
Spacing of transverse reinforcement (mm)	Capacity of column (KN)	Percentage difference	PEF load (KN)	%ge difference
100	150.493	reference	141.136	reference
200	143.601	4.6	137.453	2.61
300	140.674	6.52	135.023	4.33

Table 9 Peak lateral load resistance of columns with different spacing of transverse reinforcement (f'c-45Mpa)

Spacing of transverse reinforcement (mm)	Capacity of column (KN)	%ge difference
100	147.997	Reference
200	144.09	2.64
300	141.383	4.47

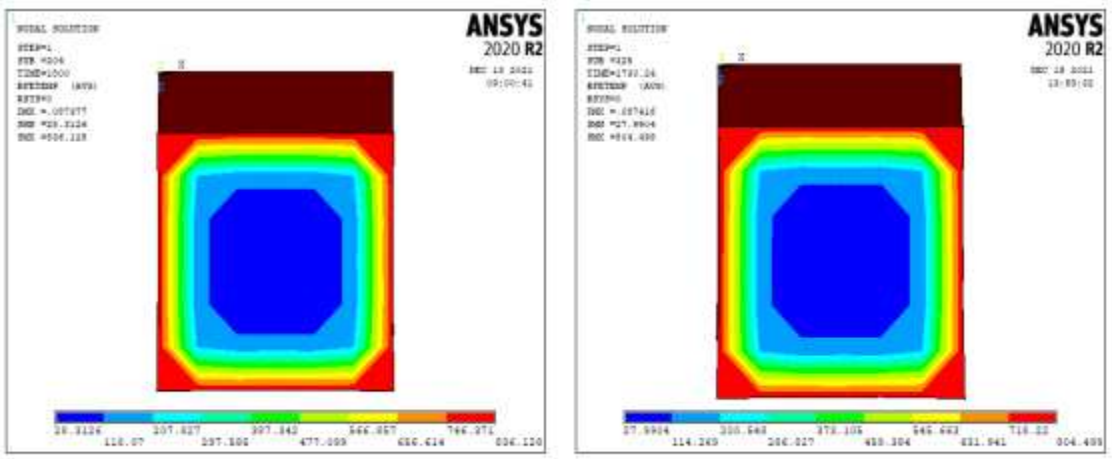
II. Damage of concrete

As shown in Fig. 13 the distribution of the color (cracks) and the amount of area covered by the damage is different for columns having different spacing of transverse reinforcement. Spacing of transverse reinforcement increases from 100mm to 300mm the damage of the column also increased. But as shown in Fig. 14 the column at 200mm and 300mm spacing of transverse reinforcement the temperature distribution is low compared to the reference spacing.



a/ Total damage of concrete (100mm) b/ Total damage of concrete (200mm)

Fig. 13 Total of the columns with different spacing of transverse reinforcement



a/ Temperature distribution (100mm)b/ Temperature distribution with (200mm and 300mm)

Fig. 14 Temperature distributions of columns with different spacing of transverse reinforcement

III. Ductility

The results presented both in Table 10 and 11 indicate that increasing the spacing of transverse reinforcement generally reduces the ductility of the reinforced concrete columns. For the column with f'c-23 MPa, the ductility ratio decreased from 7.22 at 100 mm spacing to 7.158 at 200 mm and 4.657 at 300 mm, with a significant reduction at 300 mm spacing. For the f'c-36Mpa columns, the ductility ratio decreased from 7.32 at 100 mm to 7.298 at 200 mm and 7.055 at 300 mm,

indicating a relatively small reduction. The greater spacing reduces the confinement provided by the transverse reinforcement, thereby limiting the column's ability to undergo deformation after yielding and increasing its susceptibility to brittle behavior. The results further indicate that the effect of reinforcement spacing on ductility is more significant for the 23 MPa concrete than for the 36 MPa concrete, demonstrating the importance of adequate transverse reinforcement confinement in maintaining ductile column behavior.

Table 10 Ductility ratio for different spacing of confining reinforcement (f'c-23Mpa)

Spacing of transverse reinforcement (mm)	Δu (mm)	Δy (mm)	μ = Δu/Δy
100	84	11.634	7.22
200	82.4	11.512	7.158
300	53.1	11.402	4.657

Table 11 Ductility ratio for different spacing of confining reinforcement (f'c-36Mpa)

Spacing of transverse reinforcement (mm)	Δu (mm)	Δy (mm)	μ = Δu/Δy
100	84	11.47	7.32
200	84	11.51	7.298
300	80.7	11.439	7.055

5. Conclusions

A nonlinear finite element model was developed in ANSYS Mechanical APDL to investigate the behavior of reinforced concrete columns subjected to post-earthquake fire (PEF). The model was validated against experimental results and subsequently used to evaluate the effects of confining-tie configuration, concrete strength, and transverse reinforcement spacing. Based on the numerical results, the following conclusions are drawn:

- The FE model showed good agreement with the experimental results, with a 5.67% difference in load-carrying capacity, demonstrating its suitability for investigating RC columns under PEF conditions.

- The use of intermediate confining ties increased the ultimate load-carrying capacity by 12.48% compared with the reference column, demonstrating the beneficial effect of enhanced confinement.

- Increasing the concrete compressive strength from 23 to 45 MPa increased the load-carrying capacity by 14.74%. In contrast, increasing transverse reinforcement spacing from 100 to 300 mm reduced the capacity by 6.52% under lateral loading and 4.33% under PEF loading.

- Thermal effects reduced the load-carrying capacity by 6.38% for columns with intermediate ties and 12.50% for columns without intermediate ties, indicating the importance of additional confinement under elevated-temperature conditions.

- The load-carrying capacity of the columns under PEF loading was consistently lower than that under lateral loading, primarily due to the detrimental effects of elevated temperature on the concrete and reinforcement.

- Temperature decreased progressively from the exposed outer surface toward the inner core of the columns. The reinforcing steel temperature remained below its critical temperature in the investigated cases, indicating that the concrete cover provided effective thermal protection to the reinforcement.

Author Contributions

- Selamawit Ayal Chanie conceived the study, developed the methodology, performed the numerical modeling and simulations, conducted the data analysis and interpretation, prepared the figures, and wrote the original manuscript. Tesfaye Alemu Mohammed contributed to the conceptualization, supervision. methodological guidance, validation guidance, and interpretation of results. Emebet Fentahun Ejigu, Rakev Afework Weldemichael, Getasew Kindie Mihiretu, Yeshihareg Alelign Demissie, and Feven Tadese

Geremew contributed to conceptualization, methodological guidance, technical discussions, interpretation of results, and editing of the manuscript. All authors reviewed and approved the final manuscript and agreed to be accountable for the work.

Declaration Statement

Ethical Approval and Accordance

- Not applicable. This study involved numerical finite element simulations and did not involve human participants or animals.

Consent to Participate

- Not applicable.

Consent to Publish

- Not applicable.

Data Availability Statement

- The data supporting the findings of this study are available from the corresponding author upon reasonable request.

Funding Support

- The authors received no funding from any organization or agency for the conduct of this research.

Conflicts of Interest

- The authors declares no conflicts of interest.

REFERENCE

[1] Behnam, B. and Ronagh, H. (2013). "Performance of reinforced concrete structures subjected to fire following earthquake." European Journal of Environmental and Civil Engineering, 17(4), 270–292. < http://dx.doi.org/10.1080/19648189.2013.783882

[2] Demir, U.,Goksu, C.,Unal, G., Green, M., and Ilki, A. (2020). "Effect of Fire Damage on Seismic Behavior of Cast-in-Place Reinforced Concrete Columns." Journal of Structural Engineering, 146(11). < https://doi.org/10.1061/(ASCE)ST.1943-541X.0002794

[3] Imani, R. Mosqueda, G. and M. Bruneau, F. (2015). "Experimental Study on Post-Earthquake Fire Resistance of Ductile Concrete-Filled Double-Skin Tube Columns."Journal of Structural Engineering, 141(8). < http://dx.doi.org/10.1061/(ASCE)ST.1943-541X.0001168

[4] Kamath, P., Sharma, U. K., Kumar, V.,Bhargava, P., Usmani, A., Singh, B., Singh, Y., Torero, J., Gillie, M. and Pankaj, p. (2015). "Full-scale fire test on an earthquake-damaged reinforced concrete frame." Fire safety journal, 73,1-19. < http://dx.doi.org/10.1016/j.firesaf.2015.02.013

[5] Shah, A. H., Sharma, U.K. and Bhargava, P. (2017), "Banthia-Basheer Special Issue on Advances in Science and Technology of Concrete Outcomes of major research on full scale testing of RC frames in post-earthquake fire." Construction and Building Materials 155, 1224–1241. < http://dx.doi.org/10.1016/j.conbuildmat.2017.07.100

[6] Vitorino, H., Rodrigues, H. and Couto, C. (2020). "Evaluation of post-earthquake fire capacity of reinforced concrete elements." Soil dynamics and earthquake engineering, 128. < https://doi.org/10.1016/j.soildyn.2019.105900

[7] Kodur, V., Dwaikat, M. and Raut, N. (2009). "Macroscopic FE model for tracing the fire response of reinforced concrete structures." Engineering structures, 31, 2368–2379. (http://dx.doi.org/10.1016/j.engstruct.2009.05.018).

[8] Vitorino, H., Vila Real, P., Couto, C., & Rodrigues, H. (2022). Post-earthquake fire assessment of reinforced concrete frame structures. *Journal of Structural Fire Engineering*. https://doi.org/10.1080/10168664.2022.2062084

[9] Ni, S. and Birely, A. C. (2018). "Impact of p hysical seismic damage on the fire resistance of reinforced concrete walls." Construction and Building Materials, 182, 469–482. < https://doi.org/10.1016/j.conbuildmat.2018.06.120

[10] Han, S., Xiao, G., Tan, W., Mai, P., Zhou, A., Yu, J., & Ou, J. (2024). Effect of tie parameters on strength and ductility of concrete columns reinforced with hybrid steel-fiber reinforced polymer (FRP) composite bars. Engineering Structures, 319, 119051. https://doi.org/10.1016/j.engstruct.2024.119051

[11] Buch, S. H., & Sharma, U. K. (2026). Behaviour of tie confined reinforced concrete columns subjected to standard fire exposure. Advances in Structural Engineering, 29(3), 491–513. https://doi.org/10.1177/13694332251353621

[12] Elbakry, H. M., Ebeido, T. I., El-Tony, E.-T. M., & Ali, M. M. (2024). Behavior of RC columns with different internal ties configurations subjected to axial load: Numerical study. Journal of Civil Engineering and Construction, 13(4). https://doi.org/10.32732/jcec.2024.13.4.192

[13] Dashti, S., Caglayan, B. O., & Dashti, N. (2025). *Post-Earthquake Fire Resistance in Structures: A Review of Current Research and Future Directions*. *Appl. Sci.* **2025**, *15*(6), 3311; https://doi.org/10.3390/app15063311

[14] Düzgün, O. A., & Küçük, E. N. *Post-fire seismic performance of reinforced concrete structures*. https://doi.org/10.1016/j.istruc.2023.105718